We are IntechOpen, the world's leading publisher of Open Access books Built by scientists, for scientists

4,800
Open access books available

122,000
International authors and editors

135M
Downloads

Our authors are among the

154
Countries delivered to

TOP 1%
most cited scientists

12.2%
Contributors from top 500 universities

CLARIVATE ANALYTICS BOOK CITATION INDEX INDEXED

WEB OF SCIENCE™

Selection of our books indexed in the Book Citation Index in Web of Science™ Core Collection (BKCI)

Interested in publishing with us?
Contact book.department@intechopen.com

Numbers displayed above are based on latest data collected.
For more information visit www.intechopen.com

18

Mechanisms of Microstructure Control in Conventional Sintering

Adriana Scoton Antonio Chinelatto[1],
Elíria Maria de Jesus Agnolon Pallone[2],
Ana Maria de Souza[1], Milena Kowalczuk Manosso[1],
Adilson Luiz Chinelatto[1] and Roberto Tomasi[3]
[1]*Department of Materials Engineering - State University of Ponta Grossa*
[2]*Department of Basic Sciences – FZEA - São Paulo University*
[3]*Department of Materials Engineering - Federal University of São Carlos*
Brazil

1. Introduction

The manner and mechanisms involved on the sintering process are essential investigation to achieve the required microstructure and final properties in solids. During the conventional sintering of a compacted powder, densification and grain growth occur simultaneously through atomic diffusion mechanisms. Many researchers have been working on reducing the grain size below 1 μm aiming to improve some properties, such as strength, toughness and wear resistance in ceramics (Greer, 1998; Inoue & Masumoto, 1993; Morris, 1998). In order to obtain ultra-fine ceramic microstructures, nanocrystalline powders can be used. Although the sinterability of nanoparticles is superior to that of fine particles due to the higher sintering stress, densification of these powders is often accompanied by grain growth (Suryanarayana, 1995).

Hot pressing sintering (He & Ma, 2000; Porat et al., 1996), spark plasma sintering (Gao et al., 2000; Chakravarty et al., 2008) or pulse electric current sintering (Zhou et al., 2004) are typical techniques employed to produce nanostructured ceramics. However, many of these techniques are not economically viable depending on the use of the final product. Thus, conventional pressureless sintering is still a more attractive sintering method to produce ceramic products, mainly due to its simplicity and cost compared to other methods. In the conventional pressureless sintering, a controlled grain size with high densification could be achieved by adequate control procedures of the heating curve — herein defined as the maximization of the final density with minimum grain growth.

One hypothesis to the heating curve control can be achieved by improving the narrowing of grain size distribution in a pre-densification sintering stage followed by a final densification stage namely at a maximum densification rate temperature (Chu et al., 1991; Lin & DeJonghe, 1997a, 1997b). In a thermodynamics point-of-view, another hypothesis is regarded to control the heating schedule at temperature ranging the active grain boundary diffusion. Note, however, that the grain boundary migration is sufficiently sluggish and the

densification could occur without grain growth. The aforementioned hypothesis was proposed by Chen and Wang (Chen & Wang, 2000) and has been successfully applied to different types of materials. A second phase can be added to preserve fine grains. In this case, grain boundary inhibition can be due to the pinning effect, which is associated with particles locations at grain boundaries or triple junctions (Chaim e al. 1998; Trombini et al., 2007). This drag pinning effect associated with heating curve control can be more effective to suppress the grain growth.

2. Nanostructure materials

The size control of microstructural elements has been always considered as one of the most important factors in control of several properties in the development of new materials or design new microstructures. As a historical example, it can be mentioned that the grain refining of metallic materials, which results in increased mechanical strength, tenacity, occurrence of superplastic, etc. New materials with sub-micron grain size have been developed recently as commercial materials and the latest generation of this development is the nanostructured materials (Inoue & Masumoto, 1993).

Nanostructured materials (also called nanocrystalline materials, nanophasics materials or nanometer-sized crystalline solids) are known to have properties or combinations of properties, which may be new or even superior to conventional materials (Greer, 1998). Nanostructured materials can be defined as a system containing at least one microstructural nano characteristic (with sizes ranging up to 100-150nm). Due the extremely small dimensions, a large volume fractions atoms located in grain boundaries (Morris, 1998), which gives them a unique combination of composition and microstructure (Suryanarayana, 1995). Generally, these materials exhibit high strength and hardness, increased diffusivity, improved ductility and toughness, reduced elastic modulus, lower thermal conductivity when compared to larger grain size materials (~10μm) (Suryanarayana, 1995).

Since nanocrystalline materials contain a large fraction of atoms in grain boundaries, many of these interfaces provide high density of short diffusion paths. Therefore, it is expected that these materials show increased diffusivity compared to polycrystalline materials of the same composition and conventional particle size (of the order of microns) (He & Ma, 2000). The consequence of such increased diffusivity is increased sinterability of nanometric powders, which causes decrease in sintering temperature of these powders when compared to the same material with conventional particle size (Porat et al., 1996).

The driving force for sintering or "sintering stress" of nanocrystalline ceramics with pores in the range of 5nm is about 400MPa (considering γ about $1Jm^{-2}$), while for conventional ceramics with pores around 1 μm it is 2 MPa. Thus, a nanocrystalline ceramic must have a great thermodynamic driving force for retraction, which must densify extremely well even under unfavorable kinetic conditions such as low temperatures (Suryanarayana, 1995).

The interest in this nanostructured materials area has grown due to the availability of nanocrystalline ceramic powders. These nanocrystalline powders can be synthesized using different techniques, but its consolidation into dense ceramics without significant grain growth is still a challenge.

Compaction and sintering of ultra fine and/or nanoscale powder have a positive set of aspects over behavior during processing and final properties of products; however, there are also

several processing difficulties. Main positive aspects include: increased reactivity between reagents and solid particles and between particles and the gas phase, which are important processes in synthesis; increased sintering rate and particularly lowering of sintering temperature, which can reduced by half the material's melting point (Hahn, 1993; Mayo, 1996).

On the other hand, also due to the large surface area and large excess of free energy nanometric powder systems, there are many detrimental aspects to the processing and obtaining the refined and homogeneous microstructures. Some of these aspects are: a very strong tendency to agglomeration of primary particles of nanometric powders; difficulties of mixing and homogenization of compression due to the strong attraction between particles; demand for greater sintering atmosphere control, not only due to the higher reactivity, but also the possibility of formation of thermodynamically unstable phases and appearance of strong effect of adsorbed gases on the surface (Allen et al., 1996; Averback et al., 1992).

Many studies (Chen & Chen, 1996, 1997) on nanometric size particles have shown reduction of sintering temperature. Hahn et al. (Hanh, 1990), studying the sintering of nanometric TiO_2 (12nm), Y_2O_3 (4 nm) and ZrO_2 (8nm), found lower sintering temperatures than those conventional. The sintering of TiO_2 occurred at 1000°C while conventional TiO_2 sintering requires temperatures above 1400°C. The same pattern of reduced sintering temperature was observed for Y_2O_3 and ZrO_2. In spite of the proven decrease in sintering temperature of nanometric powders, its densification is often accompanied by a large grain growth, causing lost of their nanocrystalline ceramics characteristics.

2.1 Effect of heating curve in the sintering

Production of polycrystalline ceramics with high density and small grain size have been studied for several processing routes. Among these routes may be cited: colloidal processes of powder with controlled particle size distribution (Sigmund & Bergström, 2000; Lim et al., 1997), sintering under pressure (He & Ma, 2000; Weibel et al.,1997), use of additives incorporated into a second phase or in solid solution (Novkov, 2006; Erkalfa et al., 1996), spark plasma sintering (Gao et al., 2000; Chakravarty et al., 2008, Bernard-Granger & Guizard, 2007), pulse electric current sintering (Zhou et al., 2004), etc. Usually these methods have several limitations on usage, in addition to requiring more complex and expensive equipment. Thus, sintering without pressure is even a more desirable sintering method to produce ceramic products, mainly due to its simplicity and cost when compared to other methods.

In pressureless sintering, beyond the control of powders' characteristics, control of the sintering process has a major effect on final material's density and microstructure. This method is often unable to prepare dense ceramics with ultrafine grain size, once way the final sintering stage, both densification and grain growth occur by the same diffusion mechanisms (Mazahery et al., 2009).

Heating curve control to manipulate the microstructure during sintering is a route that has been studied and offers advantages such as simplicity and economy. The rate-controlled sintering (Brook, 1982, German, 1996) is one of the ways in which the relationship between densification rate and grain growth rate is determined to identify the sintering temperature at which densification rate is maximized (Chu et al., 1991). Ragulya and Skoroklod (Ragulya & Skoroklod, 1995) studied the rate-controlled sintering of ultra fine nickel powders

obtaining sintered samples with high densities (~ 99% TD) and grain size smaller than 100nm. Based on their results, they stated that rate-controlled sintering is a possible route for obtaining dense materials with nanocrystalline structure.

A direct consequence of the rate-controlled sintering method is fast firing (Harmer & Brook, 1981), which can produce dense materials with small grain size, minimizing the time of exposure at temperatures where grain growth is fast compared with densification (Chu et al., 1991). This is possible because, generally, coalescence mechanisms (eg, surface diffusion and vapor transport) prevail over densification mechanisms (eg, volumetric diffusion by grain boundary diffusion) at low temperatures. In this case, shorter times at lower temperatures reduce growth, so that the driving force for densification is not decreased significantly (Lin & DeJonghe, 1997). In case of alumina (Harmer et al., 1979) for example, the activation energy for densification is greater than that for grain growth, and high sintering temperatures the most suitable (Harmer & Brook, 1981).

Kim and Kim (Kim & Kim, 1993) studying the effect of heating rate on shrinkage of pores in yttria-zirconia doped, stated that growth of pores is also inhibited by the fast firing process, helping thus to increase the densification. Searcy (Beruto et al., 1989; Searcy, 1987) suggested that the beneficial effects attributed to the fast firing may be due in part to temperature gradients developed in the sample during heating.

Rate-controlled sintering is more efficient for non-agglomerated powders, in which the microstructure develops relatively homogeneous. However, benefits of these techniques have proved less effective for agglomerated systems. The difficulty of obtaining homogeneous green microstructures using ultra-fine powders, owing to their high degree of agglomeration leads to inhomogeneous, low densification rate and limited final density (Rosen & Bowen, 1988; Inada et al. 1990; Dynys & Hallonen, 1984).

Recently, the availability of many different production routes for ultrafine and nanosized ceramic powders have led research to focus increasingly on the processing of these types of powders. Transformation processes that occur at low temperatures have been observed and studied particularly before or at the beginning of the densification stages of sintering. These processes, which have been reported for coarsening and particle repacking (Chen & Chen, 1996, 1997), affect the subsequent sintering stages. When these processes are controlled, it is possible to obtain dense and fine microstructures. One way to control these processes is optimizing the material's heating curve by pre-treating it at low temperatures.

De Jonghe et al. (Chu et al., 1991; Lin & DeJonghe, 1997a, 1997b) found that pre-heat treatment (50 to 100 hours) at low temperatures (800 ºC), in which little or no densification occurs, can improve densification and microstructure of a high purity alumina with and without MgO addition. A consequence of these pre-treatments was reducing the densification rate in the initial stages of sintering. However, benefits of evolving a more homogeneous microstructure are evidenced in the final stages of sintering, allowing a final microstructure refinement. According to DeJonghe et al. (Chu et al., 1991; Lin & DeJonghe, 1997a, 1997b), the pre-treatment leads to more compaction due to the strong increase in the neck formation among particles, promotes the elimination of fine particles, probably through the ripening process of Ostvald and produces a narrower distribution in pore size. These factors make decrease the density fluctuation during sintering, thus favoring the achievement of more uniform microstructures. The best microstructural homogeneity, both

in relation to pores and particles, retards the closing of the pore network, so that pores remain open until higher densities inhibiting grain growth more effectively (Lin & DeJonghe, 1997b).

Kim and Kishi (Kim & Kishi, 1996) observed the effect of pre-treatments on strength and subcritical crack growth in alumina. Alumina sintered by hot pressing had 400-500MPa resistance while alumina subjected to a pre-treatment (1000 to 1200 ^{o}C for 10 hours) increased their resistance to 750MPa. They concluded that the fracture toughness of grain boundary is increased with pre-treatment and toughness of grain boundary reduces the rate of subcritical crack growth sintering resulting in increased strength of the material. Sato and Carry (Sato & Carry, 1995) studied the effect of particle size and pre-treatment on ultra-fine alumina and found that the pre-treatment delays the start of abnormal grain growth, creating a more uniform microstructure before densification. Chinelatto et al. (Chinelatto et al., 2008) studied the influence of heating curve on the sintering of alumina subjected to high-energy milling and observed that the isothermal treatments at a temperature below the beginning of linear shrinkage cause the fine particles to disappear, narrowing the final grain size distribution.

A new sintering process in two steps was proposed by Chen (Chen & Wang, 2000). The author showed the possibility of obtaining fully dense bodies and sizes of nanosized grains in sintering without applying pressure. This rapid sintering technique inhibits grain growth that occurs in the final stages of sintering and consists of a heating curve in which the ceramic body is subjected to a rapid peak in temperature followed by cooling to the sintering level. Thus, there is densification of the material without the characteristic grain growth. Suppression of grain growth in the final stage of sintering was achieved by exploiting the difference between the kinetics of diffusion in the grain boundary and controlled grain boundary migration rate. Chen and colleagues used the technique of two-step sintering nanosized powders of Y_2O_3 (Wang et al., 2006a), $BaTiO_3$ ferrites and Ni-Cu-Zn (Wang et al., 2006b). Other studies are reported in the literature using the two-step sintering to post nanometric TiO_2 (Mazaheri, 2008a), yttria stabilized zirconia (Mazaheri, 2008b), zirconia (Tartaj, 2009), abrasive alumina with additions of MgO-CaO-SiO_2 (Li et al., 2008), alumina-zirconia (Wang et. al., 2009) among others.

According to Chen and Wang (Chen & Wang, 2000; Wang et al., 2006a), in a temperature range called kinetic window, occurs by grain boundary or volumetric diffusion while the grain boundary movement is restricted, so that the densification occurs without, however, growth occurs grain. The sintering temperature in this region results in elimination of residual porosity without grain growth at final stage of work. Suppression of grain growth but not densification is consistent with a network of grain boundaries anchored by triple junction points, which have higher activation energy for migration than grain boundaries (Wang et al., 2006a).

The choice of temperature for both steps is essential for successful sintering. If densities greater than a critical value are reached in the first heating stage, the density of triple junctions decreases, so the effect of the triple points drag mechanism is reduced and the grain growth control is injured in the final sintering stages. On the other hand, if densities are lower than certain critical value, it is not possible to achieve material's densification in the second sintering stage (Chen & Wang, 2000; Hesabi et al., 2009).

Zhou et al. (Zhou et al., 2003) showed that triple junction at large grain sizes is not significant since its volume fraction is negligible compared with the total interface fraction. It is believed that occurs when the passage to the second stage of sintering, the energy in the triple junction during the whole period of time, remains constant. If there is increase in temperature it may be due to increased energy of the system, so there may be a greater mobility of the triple junction in comparison with the grain boundary, so the contour can move freely without any difficulty, indicating a common growth grain. At low temperature, the triple junctions make difficult the movement of grain boundaries not allowing grain growth occurrence (Czubayko et al., 1998).

Nanometric and sub-micrometric alumina powders (Hesabi et al., 2009; Li & Ye, 2006) were also sintered in two steps. Ye and Li (Li & Ye, 2006) found that it is necessary that nanosized alumina powders reach 85% theoretical density in the first stage of sintering, so it can be fully densified at the second level, while Bodisova (Bodisova et al., 2007) showed that density should not be less than 92% theoretical density to achieve full densification without grain growth in the second level for post sub-micron alumina.

2.2 Addition of particles of a second phase

A strategy used to achieve nanometric grain sizes is through addition of solutes or particles of a second phase in single-phase ceramics, which reduce the grain boundary mobility or fix the grain boundary, respectively (Novkov, 2006). This strategy has been used successfully by many researchers. Chaim et al. (Chaim et al., 1998) added 4 wt% trivalent oxides (Y, La, Bi) and tetravalent oxides (Ce, Th) in nanocrystalline zirconia powder and found that Y_2O_3, CeO_2 and ThO_2 inhibit grain growth during sintering. According to Mayo (Mayo, 1996), Hahn et al. added to a powder Y_2O_3 nanocrystalline TiO_2 to limit grain growth. Part of Y_2O_3 dissolved in the regions of grain boundaries and partly reacted with TiO_2 to form a second phase in grain boundaries. These two effects have limited the growth of grains so that the Y_2O_3 sintered without applying pressure reached 90% density with 50nm grain size and Y_2O_3; when adding TiO_2, sintered under the same conditions, it showed 30nm grain size with 99% density.

Recent studies have shown that grain growth inhibition during sintering, which favors increase in mechanical properties of the nanocomposite, occurs by adding small amounts of nanosized zirconia inclusions in a ceramic body of alumina matrix. Grain growth inhibition has also been observed with nanometric inclusions of silicon carbide. However, densification during sintering is difficult by the presence of zirconia in alumina. Other problems were reported in the literature: tendency to particles agglomeration and difficulty to dispersion of nanosized particles of zirconia in alumina matrix, particularly for mechanical mixing methods (Sakka & Hiraga, 1999; Susuki, 2001).

Trombini et al. (Trombini et al., 2007) dispersed powder of alumina and zirconia separately, which allowed them to obtain a complete and homogeneous dispersion of nanosized particles of zirconia in alumina matrix. The Spark Plasma Sintering (SPS) could be used to obtain samples with densities close to theoretical density with very homogeneous microstructure and grain size similar to the initial particle size of powder with at 1300 ºC sintering temperature. Pierri et al. (Pierri et al., 2005) observed that the presence of small amounts of zirconia (1 vol%) was sufficient to cause an grain growth inhibition of alumina,

allowing the sintering process without application of pressure that results in higher final densities and increased mechanical strength and wear resistance.

3. Experimental procedure

Initially, the alumina powder was processed to remove the hard agglomerates. The following procedure was used: powder was dispersed in isopropyl alcohol with 0.2 w% of PABA (4-aminobenzoic acid) and 0.5 w% of oleic acid. The suspension was submitted to a ball mill during 10 h, using zirconia balls (ball/powder in mass ratio of 2:1) in a polypropylene vial. Suspension was dried at 75ºCand then pulverized and sieved.

For dispersion of zirconia nanometric powder in the alumina powder a ZrO_2 suspension was prepared through traditional balls milling (ZrO_2 balls with 5mm diameter) using 0.5 wt% of deflocculant PABA (4-aminobenzoic acid) in alcoholic medium with a balls/powder mass ratio of 4:1. After 12 hours milling, suspension was separated through the milling and reserved. Simultaneously, Al_2O_3 suspension in alcoholic medium was prepared with 0.2 wt% PABA with a balls/powder ratio of 5:1 for 1 hour in balls mill. 5 vol% ZrO_2 previously prepared were added to this suspension under agitation. Then, final suspension was mixed in conventional balls mill for 22 hours. Finally, 0.5w% oleic acid was added to the suspension and mixed for 2 more hours. The obtained mixtures were dried at room temperature under flowing air.

Prior to sintering experiments, samples of pure alumina were uniaxially pressed under 80 MPa into cylindrical compacts (ø=10 mm, and height of about 5 mm) and isostatically cold-pressed under 200 MPa. Samples were heat-treated at 600°C in air for 1 h to eliminate organic materials. Green density of samples was about 59% of the theoretical density (%TD).

4. Results and discussion

Conventional sintering experiments were carried out at temperature between 900 and 1500ºC in air with 2 h dwell time. This sample also was sintered in a Netzsch – DIL 402C dilatometer at 15ºC/min constant heating rate in air atmosphere. Based on these results, steps for the sintering were defined. The sintering process was performed in electric furnace (Model Lindberg) in the presence of $MoSi_2$ heating elements in air atmosphere.

In addition to thermal analysis by dilatometry, sintered samples were further characterized by the apparent density taken the Archimedes method as reference, grain size measurements using an image analysis program, and the microstructure was analyzed by scanning electronic microscopy (SEM).

Figure 1 shows the linear shrinkage rate versus temperature during heating in dilatometer at15°C/min constant heating rate. Sintering shrinkage started at 1030ºC and maximum shrinkage rate occurred at 1345ºC. In figure 1, two different areas can be defined: the first area beginning between 900ºC and 1000ºC and until approximately 1080ºC and refers to the temperature range before sample shrinkage beginning. As shrinkage is directly related to the densification of ceramic body during the sintering process, sintered samples did not begin the densification at temperatures lower than 1080ºC having a rearrangement

process, coarsening of the particles and appearance of contact points among particles. The second area can be defined as the one where shrinkage occurs, from approximately 1080˚C to 1500ºC. In this area, shrinkage rate reaches the maximum value at approximately 1350ºC.

The sintering temperature effect on the densification and grain growth of compacts sintered at temperature ranging between 900 and 1500ºC for 1 hour is shown in figure 2. No significant densification was observed below 1030ºC confirming the dilatometric results (figure 1). Densification was accelerated at the temperature between 1100ºC and 1350ºC, without, however, presenting great grain growth. At higher temperature, densification was minimal but the grain growth was fast. Final grain size of the nearly fully dense structure was higher than 1800 nm. While relative density increased from 95% to 99.2% with increase in temperature from 1300ºC to 1500ºC, the average grain size became coarser from 480 nm to 1800 nm; in other words, there was more than 250% increase in grain size.

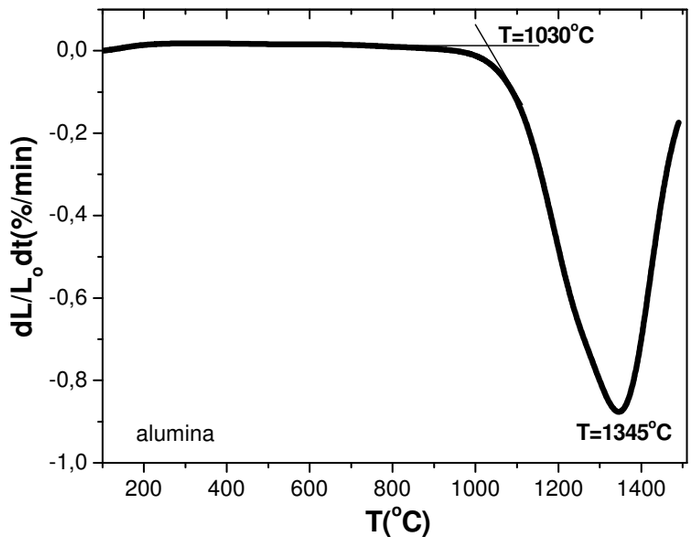

Fig. 1. Linear shrinkage rate versus temperature during heating in dilatometer at 15°C/min constant heating rate.

It has reported that dispersed open pores can pin grain boundaries and hinder grain-boundary migration in the second stage of sintering, for which the grain growth is suppressed (German, 1996). In contrast, a very sharp ascending of grain size is observable in the final sintering stage (relative density above 90% TD); however, there is remarkable increase in density. It has been confirmed that open pores referring to the intermediate stage of sintering collapse to form the closed ones after the final stage starts. Such a collapse results in a substantial decrease in pore pinning, which triggers the accelerated grain growth.

Considering the results of sintering experiments (figures 1 and 2) and to suppress the accelerated grain growth at the final sintering stage, two different sintering heating curves were applied to produce densification of Al_2O_3 compacts. These experiments were carried out using 15ºC/min heating rate.

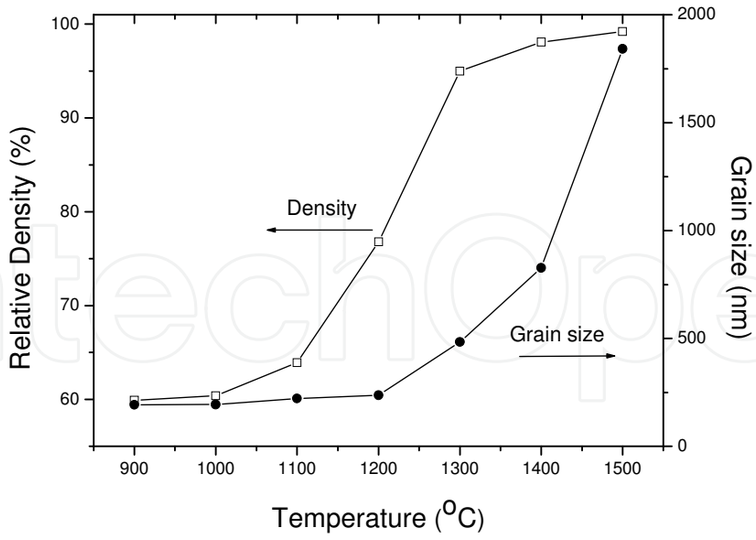

Fig. 2. Density and grain size of Al_2O_3 compacts after sintering at various temperatures for 1 hour.

In the first sintering heating curve one hypothesis was assumed: the maximization of final density with minimum grain growth could be achieved by improving the narrowing of grain size distribution at a pre-densification sintering stage and producing the final densification at a maximum densification rate. To confirm this hypothesis, a temperature below the onset of the densification process was chosen. This effect can be observed in samples with the first step at 1050ºC. Samples produced by the first step at 1050ºC followed by a second step at 1500°C showed significantly smaller final grain sizes as shown in figure 3 (Chinelatto et al., 2010).

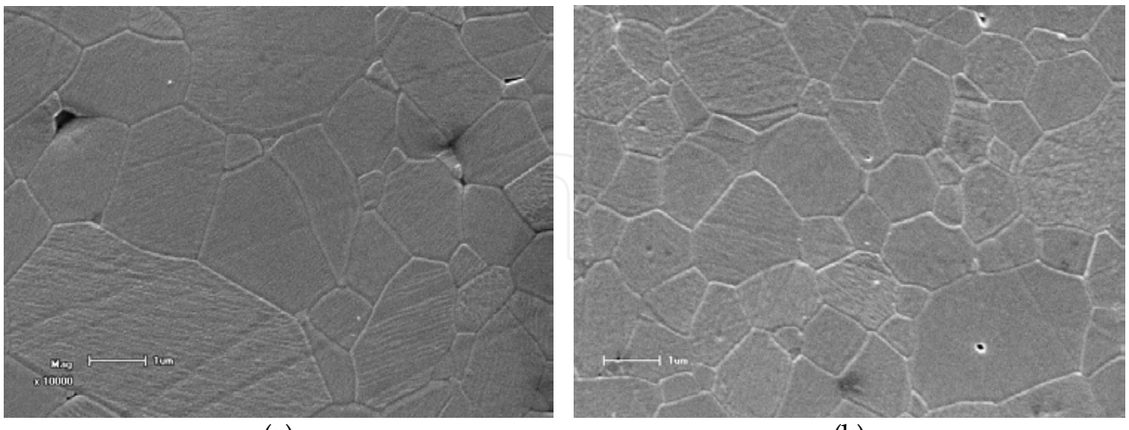

(a) (b)

Fig. 3. SEM micrographs of alumina samples after two-step sintering: a) T=1500ºC/2 h; and b) T=1050ºC/2 h and T=1500ºC/2 h.

Figure 4 shows micrographs of surface fracture of alumina compacts, one heated at 1050ºC and cooled immediately upon reaching that temperature; and the other heated to the same

temperature and kept at such temperature for 2 hours. The heat treatment made finest particles to disappear and slightly coarsened the coarsest particles, decreasing the specific surface area and slightly increasing the mean grain size as indicated in Table 1. De Jonghe et al. (Lin & DeJonghe, 1997a, 1997b) suggested that during the first step, coarsening of the microstructure by surface diffusion, vapor transport, or some combination of these mechanisms produces a more uniform microstructure by an Ostwald ripening process. The evolution to a more homogeneous microstructure can be expected from the trend of porous system to evolve towards a quasi-steady state structure. Such steady-state structural distributions are generally significantly narrower than that usually produced in a powder compact (Chu et al., 1991).

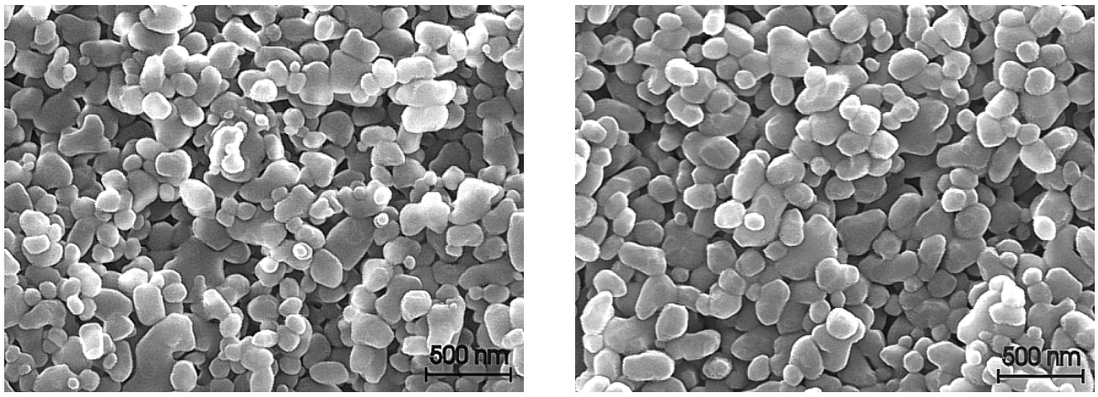

(a) (b)

Fig. 4. SEM fracture surfaces of Al_2O_3 compacts: (a) heated at 1050°C and cooled immediately e (b) heated at 1050°C for 2 hours.

	1050°C	1050°C/2 hours
Superficial area (m^2/g)	12.3	10.5
Mean grain size (nm)	119 ± 33	133 ± 28

Table 1. **Superficial area and mean grain size of particles.**

Other heating curves were developed applying sintering curves coherent with the temperature ranges in which the two processes, i.e., narrowing grain size distribution and final densification, were expected to occur. The following conditions were defined for the sintering heating curves: the first step for alumina was at 1050°C and 1000°C and the second step was at the maximum sintering temperature of 1350°C. Table 2 describes the sintering conditions and findings regarding density and average grain size of samples produced in the two-step sintering experiments.

Changes in the relative density and mean grain size with the holding time obtained are shown in Figure 5. Increased holding time results in increase of relative density and decrease in mean grain size.

Sintering procedure	Relative Density (%TD)	Mean Grain Size (nm)
TSS1 - T_1=1000°C/3h and T_2=1350°C/3h	93.8	797.4
TSS2 - T_1=1000°C/6h and T_2=1350°C/3h	94.2	763.5
TSS3 - T_1=1000°C/9h and T_2=1350°C/3h	94.6	683.5
TSS4 - T_1=1050°C/3h and T_2=1350°C/3h	93.9	717.1
TSS5- T_1=1050°C/6h and T_2=1350°C/3h	94.1	685.1
TSS6 - T_1=1050°C/9h and T_2=1350°C/3h	94.2	659.3

Table 2. **Sintering procedure and results of relative density (%TD) and mean grain size of alumina samples.**

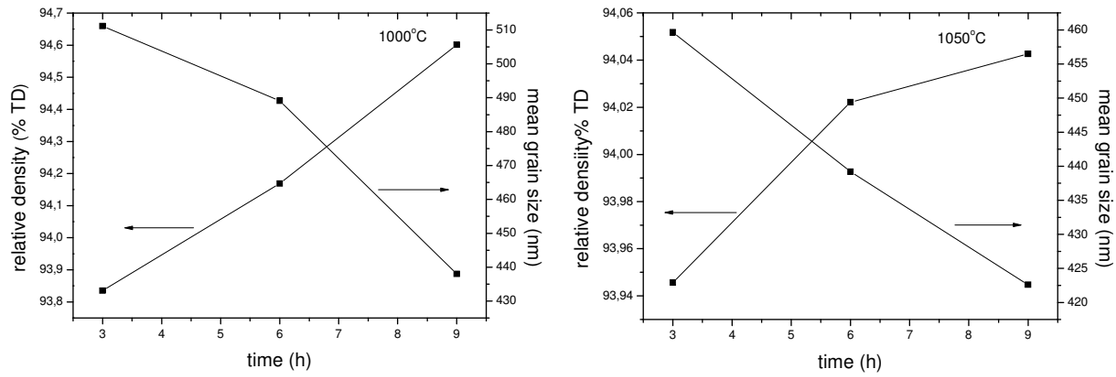

(a) (b)

Fig. 5. Relative density and mean grain size of alumina compacts sintered versus holding time at: (a) 1000°C and (b) 1050°C.

According to Lin and Dejonghe (Lin & DeJonghe, 1997a, 1997b), with the steps at low temperature, the onset of densification is delayed due to the elimination of the finest particles (and smallest pores associated with them) during the first step. The local densification associated with the finest particles in the conventional sintering is significantly reduced in compacts subjected to the first step. Thus, removal of the finest particles due to the first step reduces the differential densification and formation of densest regions in the early sintering stages. This fact causes reduction in density fluctuations in the compact and promotes a more homogeneous final microstructure.

The other two-step sintering is based on works of Chen and Wang (Chen &Wang, 2000), in which samples are first heated to a higher temperature to achieve intermediate density, and then cooled down and kept at lower temperature until they are dense. A pre-requisite for successful densification during the second step of sintering is that pores become subcritical and unstable against shrinkage.

Chen and Wang (Chen &Wang, 2000) have explained that to achieve densification without grain growth, grain-boundary diffusion needs to remain active, while the grain-boundary

migration must to be suppressed. A mechanism to inhibit grain-boundary movement is a triple-point (junction) drag. Consequently, to prevent accelerated grain growth, it is essential to decrease grain-boundary mobility. The grain growth entails a competition between grain-boundary mobility and junction mobility. Once the latter becomes less at low temperatures in which junctions are rather motionless, the mentioned drag would occur. Therefore, the grain growth is prohibited. Network mobility follows the grain-boundary mobility at high temperatures. At low temperatures, junction mobility dominates. Below the temperature at which the two rates become equal, junction mobility is essentially reduced despite the considerable grain-boundary diffusion.

Figure 2 shows that grain growth is most intense at temperatures above 1400°C. Since samples conditions after the first stage affect the second stage of sintering, grain growth resulting from heating in the first stage must be avoided. Thus, the temperature chosen for the first stage of sintering was 1400 °C.

Figure 6 shows the behavior of relative density (%TD) versus temperature for sintering at constant heating rate of alumina. Density of alumina when temperature reaches 1400°C is 81% TD. The relative density during sintering was determined from green density (dv) and measured shrinkage (ΔL/Lo), using the approximate Eq. (1), assuming that deformation is isotropic and all axial strain is devoted to specimen's densification (Ray, 1985).

$$d_i = \frac{d_v}{(1+\frac{\Delta L}{L_o})^3} \tag{1}$$

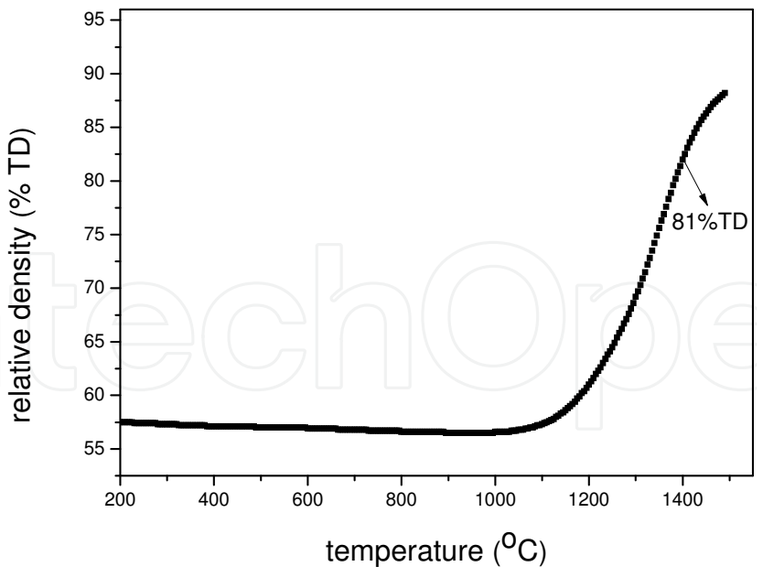

Fig. 6. Variation of relative density (% TD) versus temperature for alumina sintered at 15°C/min until the temperature of 1500 °C.

SEM micrograph of alumina when it reaches 1400°C in the first step of sintering is showed in Figure 7. The mean grain size of alumina in this condition is about 330 nm.

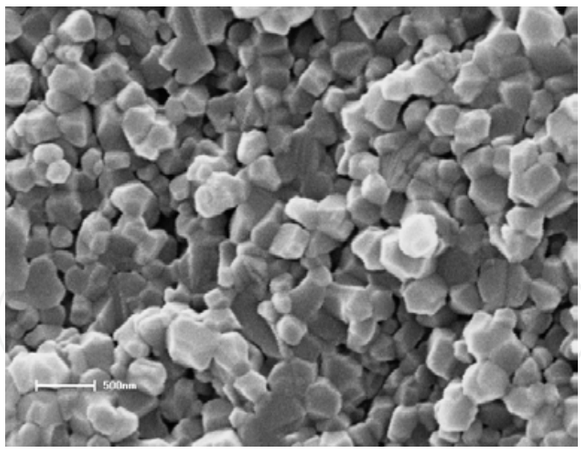

Fig. 7. SEM micrograph of alumina sintered at 1400°C.

To choose the temperature for the second step T2, it is necessary to choose a temperature in which volume diffusion or grain boundary diffusion operate while the grain boundary movement is restricted (Mazaheri et al., 2008). Therefore, the second step temperatures were 1260°C and 1300°C. Sintering conditions and results of density relative and mean grain size are presented in table 3.

Sintering procedure	Relative density (%TD)	Mean grain size (nm)
TSS7 - T_1=1400°C and T_2=1260°C/3h	91.0	518.8
TSS8 - T_1=1400°C and T_2= 1260°C/6h	92.1	579.2
TSS9 - T_1=1400°C and T_2= 1260°C/9h	93.1	647.8
TSS10 - T_1=1400°C and T_2= 1300°C/3h	95.9	668.5
TSS11 - T_1=1400°C and T_2= 1300°C/6h	96.5	692.5
TSS-12 - T_1=1400°C and T_2= 1300°C/9h	96.6	718.7

Table 3. Sintering procedure and results of relative density (%TD) and mean grain size of alumina samples.

According to the results of the second step of TSS10, TSS11 and TSS12, holding the samples at 1300°C resulted in accentuate densification. Diffusive mechanisms that seem to be time dependent are therefore active at this stage. Grain-boundary diffusion and volumetric diffusion are possibly responsible for the shrinkage of the samples. On the other hand, TSS7, TSS8 and TSS9 do not lead to a dense structure, showing the inactivity of the grain-boundary diffusion at 1260°C. Considering all these facts, one can infer that 1300°C is the minimum temperature after which the grain boundary diffusion mechanism dominates.

Due to the relatively low temperature of the second stage (1260°C), densification stops before reaching a fully dense sample. A similar trend has also been reported for the two-step sintering behavior of Y_2O_3 (Wang and Chen, 2006) and ZnO (Mazaheri et. al., 2008)

confirming that the reason for exhaustion in the second stage of densification is attributed to low temperature which retards grain-boundary diffusion as the sintering mechanism.

It can be seen in figure 8 that density variation results in increased grain size of the sample, showing that this condition is not yet the ideal to control the grain size in two-step sintering.

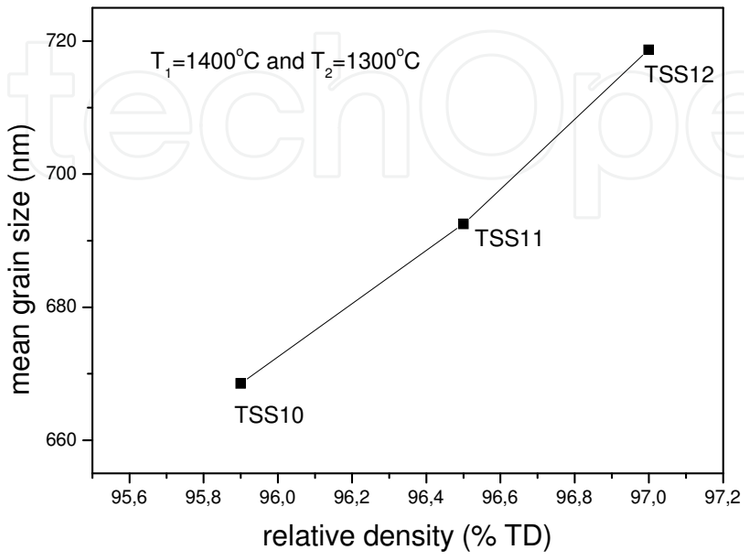

Fig. 8. Grain size/relative density trajectory obtained by two-step sintering T_1=1400°C and T_2=1300°C.

On the other hand, comparing the two-step sintering with conventional sintering, it is observed that the two-step sintering is efficient to control the grain growth. Figure 9 shows the micrographs of alumina sintered at 1500°C for 2 hours and sintered at TSS3 and TSS12 conditions.

The heating curve control, through using steps of sintering, associated with control of grain size by addition of nanometric zirconia inclusions is also control the microstrucuture in conventional sintering.

Figure 10 shows the linear shrinkage rate as function of temperature for alumina-5%vol zirconia at 15°C/min constant heating rate and 1500°C. The presence of zirconia particles increases the maximum densification rate temperature; for alumina this temperature is 1350°C (figure 1) and for alumina-zirconia the temperature is increased for 1440°C. The temperature at the beginning of shrinkage process is also altered from 1030 to 1210°C with the addition of zirconia particles. Zirconia inclusions hinder the movement of grain boundary, reducing the densification rate and grain growth (Hori et al., 1985; Liu et al., 1998; Stearns & Harmer, 1996). In the figure 11 (a) and (b), that shows the micrographs of samples of alumina-zirconia and alumina, respectively, sintered at 1500°C for 2h, the influence of zirconia on microstructure evolution is noted through observing the grain growth behavior. The addition of nanometric zirconia is very efficient to promote a controlled grain growth. The inhibitive trend is due to the pinning effect which is associated with locations of small zirconia particles at grain boundaries or triple junctions of alumina.

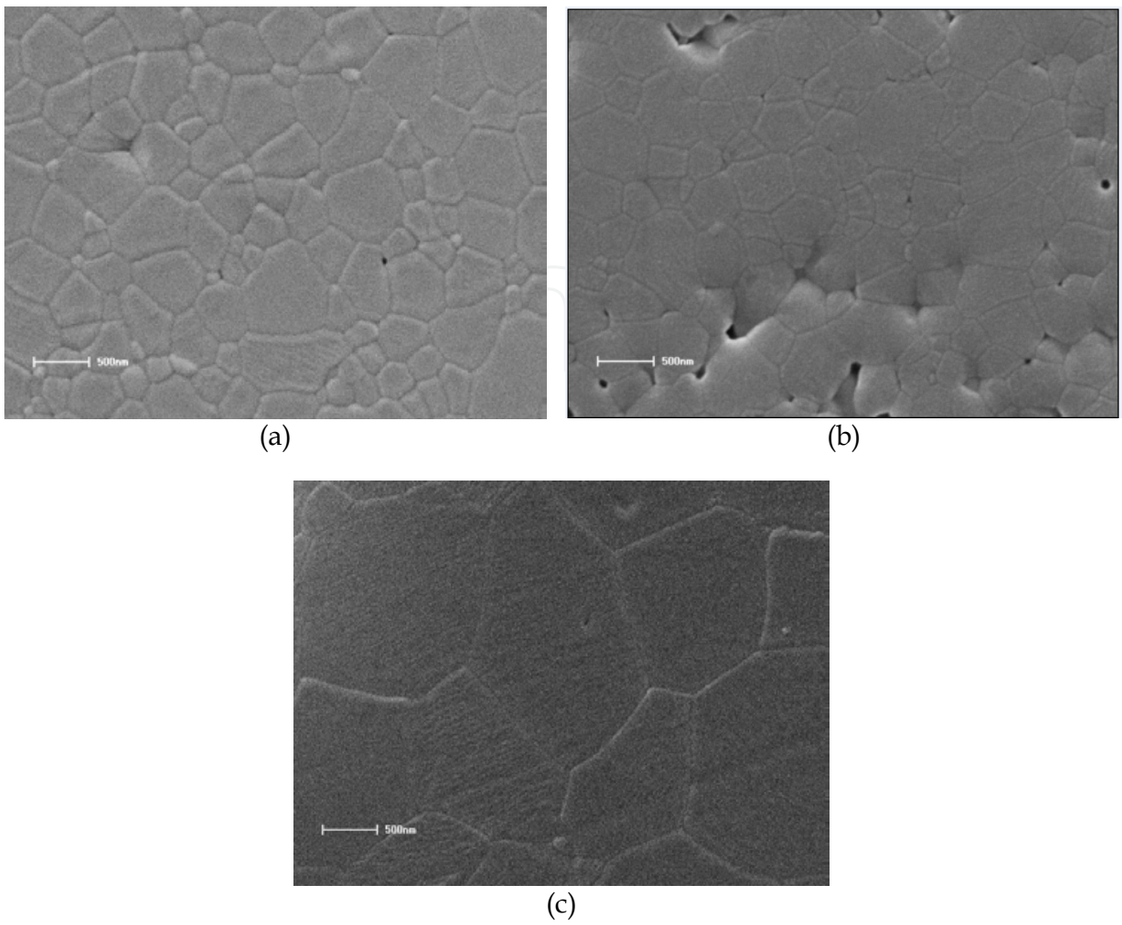

(a) (b)

(c)

Fig. 9. SEM micrographs (a) TSS3; (b) TSS12 and (c) CS.

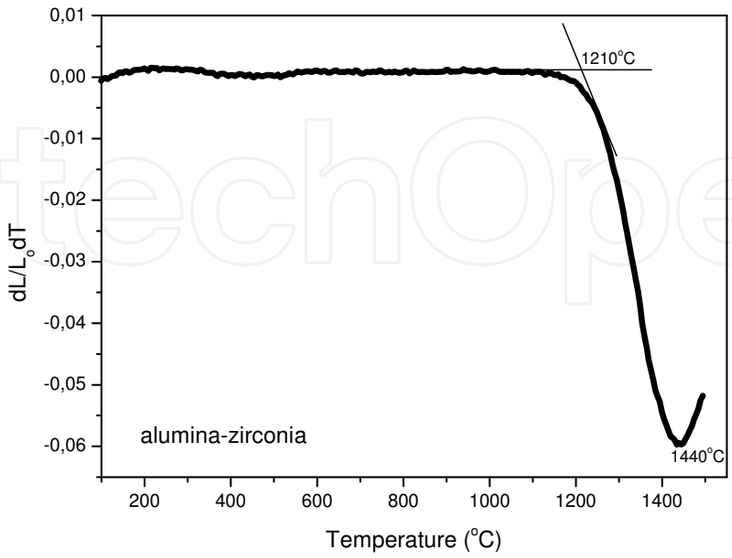

Fig. 10. Linear shrinkage rate versus temperature during heating in dilatometer at 15°C/min constant heating rate for alumina-zirconia compacts.

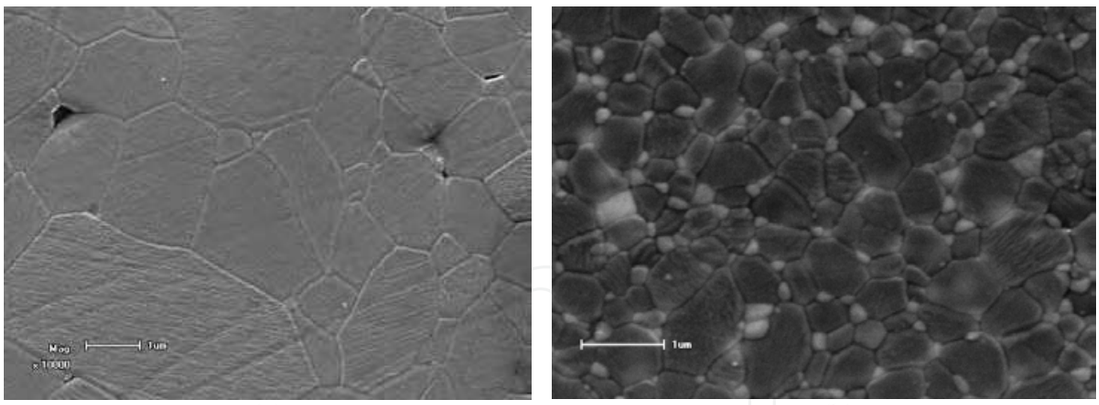

(a) (b)

Fig. 11. SEM images of sample sintered at 1500°C for 2 h: (a) alumina and (b) alumina-zirconia.

The heating curve control, combined with the presence of nanoparticles inclusions can further optimize the microstructure control. Table 4 shows the sintering procedure and results of relative density (%TD) and mean grain size for alumina-zirconia samples. Results for TSS13 and TSS14 conditions show that the two-step sintering promoted reduction of the mean grain size compared to the conventional sintering (CS1) (Manosso et al., 2010).

Sintering procedure	**Relative density (%TD)**	**Mean grain size (nm)**
CS – T=1500°C/2h	99.0	550
TSS13 - T_1=1460°C/h and T_2=1350°C/3h	97.8	330
TSS14 - T_1=1300°C/2h and T_2=1460°C/2h	99.7	410

Table 4. Sintering procedure and results of relative density (%TD) and mean grain size of alumina-zirconia samples.

The microstructure of the sample heated at 1460°C and cooled immediately and the sample sintered under TSS13 conditions are showed in Figure 12. It can be noticed an initial densification and 77%DT relative density for this sample. When the sample was heated at 1460°C and cooled down to 1350°C (TSS13 condition) the sample could be densified without grain growth (see table 2). It means that, 77% DT reached density in the first step at high temperature for this sample can be considered the critical density. In spite of the smaller grain size presented by TSS1 condition, its relative density was lower than densities of TSS14 and CS conditions. It suggests that the time of soaking in the second step can still be prolonged. Many studies (Tarjat & Trajat, 2009; Mazaheri et al., 2008) have been demonstrated that long times in the second steps allowed the total densification without grain growth.

In the TSS14 condition, pre-densification sintering stage at 1300°C for 2 hours was effective in grain growth control and final densification. Figure 13 (a), (b) and (c) presents the microstructure of alumina-zirconia sintered under CS1, TSS13 and TSS14 conditions,

respectively. These micrographs confirmed that the two-step sintering used have been efficient to the sintering process control. It can be observed that the sample conventionally sintered presents larger grain size. Finally, it was observed that the step of sintering with addition of inclusions is also efficient in grain growth.

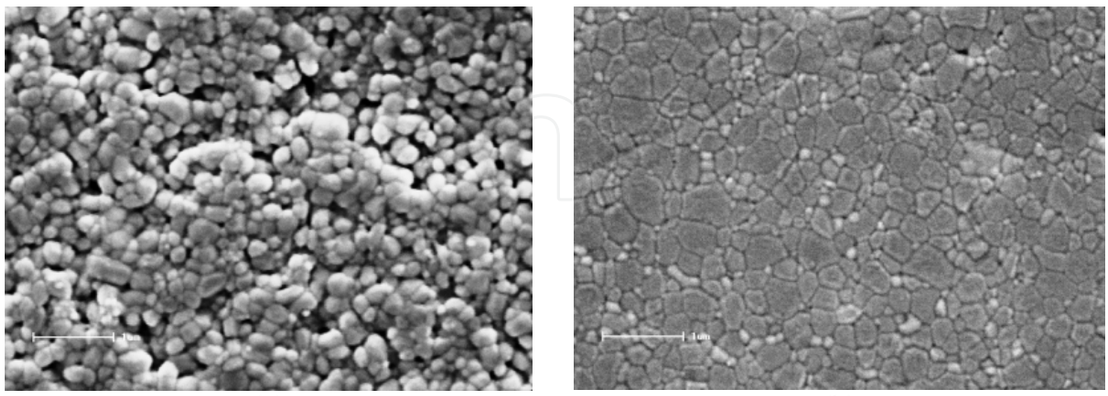

(a) (b)

Fig. 12. SEM micrographs of sintered samples: (a) T_1=1460ºC and cooled and (b) TSS13 condition.

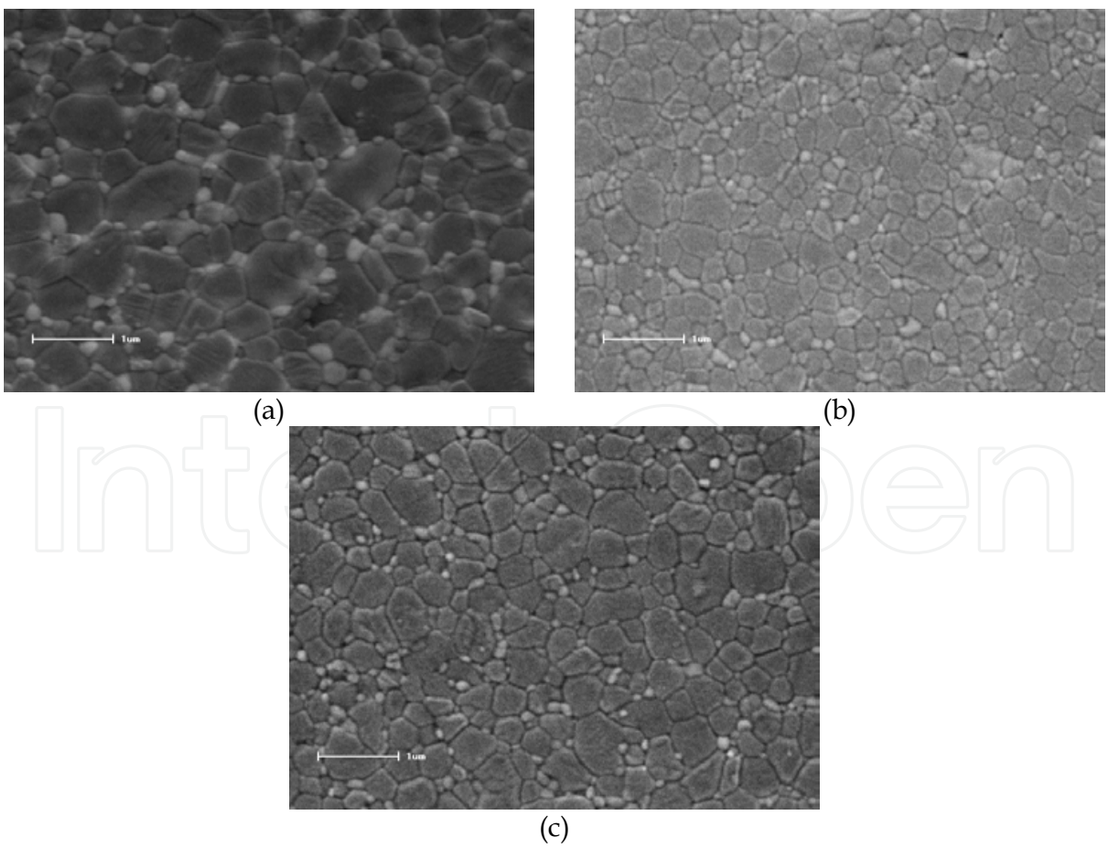

(a) (b)

(c)

Fig. 13. SEM image of the alumina-zirconia sintered under conditions: (a) CS; (b) TSS13; (c) TSS14.

5. Conclusion

The introduction of isothermal treatments in the heating curve at temperatures below the beginning of an accentuated shrinkage process influenced the development of the final microstructure, promoting a microstructural refinement of particles compacts.

The heating curve control is a simple and efficient method to control ceramic microstructure, although it is difficult to achieve an optimum condition for accessing a successful regime. The main characteristics of the heating curve control are: nanostructured ceramics can be obtained with nearly full densities; it is not necessary sophisticated and unavailable equipment, like those used for spark plasma sinterig and hot isostatic pressing; and and it is possible to achieve fully dense structures at lower temperatures.

The heating curve control, combined with the presence of nanoparticles inclusions can further optimize the microstructure control. Fine grains in the sintering induce a pinning effect on grain boundary migration and the degree of grain growth during sintering is effectively reduced.

6. References

Allen, A. J.; Krueger, S.; Skandan, G.; Long, G. L.; Hahn, H.; Kerch, H. M.; Parker, J. C. & Ali, M. N. (1996). Microstructural Evolution during the Sintering of Nanostructured Ceramic Oxides *J. Am. Ceram. Soc.*, Vol. 79, No. 5, (May 1996), pp. (1201-1212), ISSN 0002-7820.

Averback, R. S.; Höfler, H. J.; Hahn, H. & Logas, J. C. (1992). Sintering and Grain Growth in Nanocrystalline Ceramics, *Nano Mat.*, Vol. 1, No. 1, (March-April 1992) ,pp. (173-178), ISSN 0965-9773.

Bernard-Granger, G. & Guizard, C. (2007). Spark Plasma Sintering of a Commercially Available Granulated Zirconia Powder: I. Sintering Path and Hypotheses about the Mechanism(s) Controlling Densification, *Act. Mater.*, Vol. 55, No. 10, (June 2007), pp. (3493-3504), ISSN 1359-6454.

Beruto, D.; Botter, R. & Searcy, A. W. (1989). The Influence of Thermal Clycling on Densification Further: Tests of a Theory, In: Ceramic Transaction, v.1 Ceramic Powder Science IIB. Ed by Fuller, E. R. Jr.; Husner, H & Messing, G.L., pp. (911-918), Am. Ceram. Soc. Inc., ISBN: 0916094316 Westervillw, OH.

Bodisova, K.; Sajgalik, P.; Galusek, D. & Svancare, P. (2007). Two-Stage Sintering of Alumina with Submicrometer Grain Size, *J. Am. Ceram. Soc.*, Vol. 90, No. 1, (January 2007), pp. (330-332), ISSN 0002-7820.

Brook, R.J. (1982). Fabrication Principles for the Production of Ceramics with Superior Mechanical Properties, *Proc. Br. Ceram. Soc*, Vol. 32, pp. (7-24), ISSN 0524-5141.

Chaim, R.; Basat, G. & Kats-Demyanets, A. (1998). Effect of Oxide Additives on Grain Growth During Sintering of Nanocrystalline Zirconia Alloys, *Mater. Let.*, Vol. 35, No. 3-4 , (May 1998), pp. (245-250), ISSN 0167-577X.

Chakravarty, D.; Bysakh, S.; Muraleedharan, K.; Rao, T. N. & Sundaresan, R. (2008). Spark Plasma Sintering of Magnesia-Doped Alumina with High Hardness and Fracture Toughness, *J. Am. Ceram. Soc.*, Vol. 91, No. 1, (January 2008), pp. 203-208 ISSN 0002-7820.

Chen, P. L. & Chen, I. W. (1996). Sintering of Fine Oxide Powders: I, Microstructural Evolution, *J. Am. Ceram. Soc.*, Vol. 79, No. 12, (December 1996), pp. (3129-3141), ISSN 0002-7820.

Chen, P. L. & Chen, I. W. (1997). Sintering of Fine Oxide Powders: II, Sintering Mechanism, *J. Am. Ceram. Soc.*, Vol. 80, No. 3, (March 1997), pp. (637-645), ISSN 0002-7820.

Chen, I. W. & Wang, X. H. (2000). Sintering dense nanocrystalline ceramics without final-stage grain growth, *Nature*, Vol. 404, (March 2000), pp. (168-171), ISSN 0028-0826.

Chinelatto, A. S. A.; Manosso, M. K.; Pallone, E. M. J. A.; Souza, A. M. & Chinelatto, A.L. (2010). Effect of the Two-Step Sintering in the Microstructure of Ultrafine Alumina, *Adv. Sci.Tech.*, Vol. 62, (October 2010), pp. (221-226), ISSN 1662-0356.

Chinelatto,A. S. A.; Pallone, E. M. J. A.; Trombini, V. & Tomasi, R. (2008). Influence of Heating Curve on the Sintering of Alumina Subjected to High-Energy Milling. *Ceram. Int.* Vol. 34, No. 8, (December 2008), pp. (2121–2127), ISSN 0272-8842.

Chu, M.Y.; DeJonghe, L.C.; Lin, M.K.F. & Lin, F.J.T. (1991). Precoarsing to Improve Microstructure and Sintering of Powder Compacts, *J. Am. Ceram. Soc.*, Vol. 74, No 11, (November 1991), pp. (2902-2911), ISSN 0002-7820.

Czubayko, U.; Sursaeva, V.G.; Gottstein, G. & Shvindlerman, L. S. (1998). Influence of Triple Junctions on Grain Boundary Motion, *Act. Mater*. Vol. 46, No. 16, (October 1998), pp. (5863-5871), ISSN 1359-6454.

Dynys, F. W. & Hallonen, T.W. (1984). Influence of Aggregates on Sintering, *J. Am. Ceram. Soc.*, Vol. 67, No. 9, (September 1984), pp. (596-601), ISSN 0002-7820.

Erkalfa, H.; Misirk, Z. & Baykara, T. (1996). Effect of Additives on the Densification and Microstructural Development of Low-Grade Alumina Powders, *J. Mat. Proc. Tec.*, Vol. 62, No. 1-3, (November 1996), pp.(108-115), INSS 0924-0136.

Gao, L.; Hong, J. S.; Miyamoto, H & Torre, D. D. L.(2000). Bending Strength and Microstructure of Al_2O_3 Ceramics Densified by Spark Plasma Sintering, *J. Eur. Ceram. Soc.*, Vol. 20, No. 12, (November 2000), pp. (2149-2152) ISSN 0955-2219.

German, R. M. (1996). *Sintering: Theory and Practice*. Ed. John Wiley & Sons, ISBN 978-0471057864, New York.

Greer, A. L. (1998). Nanostrucuture Materials – from Fundamentals to Applications. *Mat. Sci. Forum*, Vol. 269-272, pp. (3 -10), ISSN 0255-5476.

Hahn, H. (1993). Microstrucutre and Properties of Nanostructured Oxides, *Nano. Mat.*, Vol. 2, No. 3, (May-June 1993), pp. (251-265), ISSN 0965-9773.

Hahn, H.; Logas, J & Averback, R. S. (1990). Sintering Characteristics of Nanocrytalline TiO_2, *J. Mater. Res.*, Vol. 5, No. 3, (May 1990), pp. (609-614), 1990, ISSN 0884-2914.

Harmer, M.P. & Brook, R.J. (1981). Fast Firing Microstructural Benefits, *J. Br. Ceram. Soc.*, Vol. 80, No. 5, pp. (147-48), ISSN 0307-7357.

Harmer, M. P.; Roberts, E. W. & Brook, R. J. (1979). Rapid Sintering of Pure and Doped α-Al_2O_3, *J. Br. Ceram. Soc.*, Vol. 78, No. 1, pp. (22-25), ISSN 0307-7357.

He, Z. & Ma, J. (2000). Grain Growth Rate Constant of Hot-Pressed Alumina Ceramics, *Materials Letters*, Vol. 44, No.1, (May 2000), pp.14-18, ISSN 0167-577X.

Hesabi, Z. R.; Haghighatzadeh, M. ; Mazaheri, M. ; Galusek, D. & Sadrnezhaad, S. K. (2009). Suppression of Grain Growth in Sub-Micrometer Alumina via Two-Step Sintering Method, *J. Eur. Ceram. Soc.*, Vol. 29, No. 8, (May 2009), pp. (1371-1377), ISSN 0955-2219.

Hori, S.; Kurita, R.; Yoshimura, M. & Somiya, S. (1985). Suppressed grain growth in final-stage sintering of Al2O3 with dispersed ZrO2 particles, *J. Mat. Sci. Let.*, Vol. 4, No. 9, (September 1985), pp. (1067-1070), ISSN 0261-8028.

Inada, S.; Kimura, T. & Yamaguchi, T. (1990). Effect of Green Compact Structure on the Sintering of Alumina, *Ceram. Int.*, Vol. 16, No. 6, pp. (369-373), ISSN 0272-8842.

Inoue, A. & Masumoto, T. (1993). Nanocrystalline Alloys Produced by Crystallization of Amorphous Alloys, In: *Current Topics in Amorphous Materials: Physics an Technology*, Ed. by Y.Sakurai, Y.Hamakawa, Y.Masumoto, K.Shirae and K. Suzuki, pp. (177-184), Elsevier Science Ltd, ISBN 9780-444815767, Amsterdam.

Kim, B. N. & Kiski, T. (1996). Strengthening Mechanism of Alumina Ceramics Prepared by Precoarsening Treatments, *Mat. Sci. Eng. A,* Vol. 215, No. 1-2, (September 1996), pp. (18-25). ISSN 0921-5093.

Li, J. & Ye, Y. (2006). Densification And Grain Growth of Al2O3 Nanoceramics During Pressureless Sintering, *J. Am. Ceram. Soc.*, Vol. 89, No. 1, (January 2006), pp. (139-143), ISSN 0002-7820.

Li, Z.; Li, Z; Zhang, A. & Zhu, Y. (2008). Two-Step Sintering Behavior of Sol-Gel Derived Nanocrystalline Corundum Abrasive with MgO-CaO-SiO_2 Additions, *J. Sol. Gel Sci. Technol.*, Vol. 48, No. 3, (December 2008), pp. (283-288), ISSN 0928-0707.

Liao, S. C.; Chen, Y, J; Kear, B. H. & Mayo, W. E. (1998). High Pressure/Low Temperature Sintering of Nanocrystalline Alumina, *Nano Mater.*, Vol. 10, No. 6, (August 1998), pp. (1063-1079), ISSN 0965-9773.

Lim, L. C.; Wong, P. M. & Ma, J. (1997). Colloidal Processing of Sub-Micron Alumina Powder Compacts, *J. Mat. Proc. Tec.*, Vol. 67, No. 1-3, (May 1997), pp. (137–142), INSS 0924-0136.

Lin, F. J. T. & DeJonghe, L. C. (1997a). Initial Coarsening and Microstructural Evolution of Fast-Fired and MgO-Doped Alumina, *J. Am. Ceram. Soc.*, Vol. 80, No. 11, (November 1997), pp. (2891-2896), ISSN 0002-7820.

Lin, F. J. T. & DeJonghe, L. C. (1997b). Microstructure Refinement of Sintered Alumina by Two-Step Sintering Technique, *J. Am. Ceram. Soc.*, Vol. 80, No. 10, (October 1997), pp. (2269-2277), ISSN 0002-7820.

Liu, G. L.; Qiu, H.; Todd, R.; Brook, R. J. & Guo, J. K. (1998). Processing and Mechanical Behavior of Al2O3/ZrO2 Nanocomposites, *Mat. Res. Bull.*, Vol. 33, No. 2, (February 1998), pp. (281-288), ISSN 0025-5408.

Manosso, M. K.; Pallone, E. M. J. A.; Souza, A. M.; Chinelatto, A.L. & Chinelatto, A. S. A. (2010). Two-Steps Sintering of Alumina-Zirconia Ceramics, *Mat. Sci. For.*, Vol. 660-661, (October 2010), pp. (819-825), ISSN 1662-9752.

Mayo, M. J. (1996). Processing of Nanocrystalline Ceramics from Ultrafine Particles, *Int. Mat. Rev.*, Vol. 41, No. 3, (January 1996), pp. (85-115), ISSN 0950-6608.

Mazaheri, M; Hesabi, Z. R. & Sadrnezhaad, S. K. (2008). Two-Step Sintering of Titania Nanoceramics Assisted by Anatase-to-Rutile Phase Transformation, *Scr. Mat.*, Vol. 59, No. 2, (July 2008), pp. (139-142), ISSN 1359-6462.

Mazaheri, M.; Simchi, A. & Golestani-Fardi, F. (2008). Densification and Grain Growth of Nanocrystalline 3Y-TZP During Two-Steps Sintering, *J. Eur. Ceram. Soc.*, Vol. 28, No. 15, (November 2008), pp. (2933-2939), ISSN 0955-2219.

Mazaheri, M.; Zahedi, A. M. & Sadrnezhaad, S. K. (2008). Two-Step Sintering of Nanocrystalline ZnO Compacts: Effect of Temperature on Densification and Grain Growth, *J. Am. Ceram. Soc.*, Vol. 91, No. 1, (January 2001), pp.(56-63), ISSN 0002-7820.

Mazaheri, M.; Zahedi, A. M..; Haghighatzadeh, M. & Sadrnezhaad, S.K. (2009). Sintering of Titania Nanoceramic: Densification and Grain Growth, *Ceram. Int.*, Vol. 35, No. 2, (March 2009), pp. (685-691), ISSN 0272-8842.

Morris, D. G. (1998).What Have We Learned about Nanoscale Materials? The Past and Future. *Mat. Sci. Forum*, Vol. 268-272, pp. (11-14), ISSN 0255-5476.

Novikov, V. Y. (2006). Grain Growth Controlled by Mobile Particles on Grain Boundaries, *Scr. Mat.*, Vol. 55, No. 3, (August 2006), pp.(243-246), ISSN 1359-6462.

Pierri, J. J.; Maestrelli, S. C.; Pallone, E. M. J. A. & Tomasi, R. (2005). Dispersão de Nanopartículas de ZrO_2 Visando Produção de Nanocompósitos de ZrO_2 em Matriz de Al_2O_3, *Cerâmica,* Vol. 51, No. 317, (Jan-Mar 2005), pp. (08-12), ISSN 0366-6913.

Porat, R.; Berger, S. & Rosen, A. (1996). Dilatometric Study of the Sintering Mechanism of Nanocrystalline Cemented Carbides, *Nano Mater.*, Vol. 7, No. 4, (May-June 1996) pp. (429-436), ISSN 0965-9773.

Ragulya, A.V. & Skorokhod, V.V. (1995). Rate-Controlled Sintering of Ultrafine Nickel Powder, *Nano. Mat.*, Vol. 5, No. 7-8, (September-December 1995), pp. (835-843), ISSN 0965-9773.

Rosen, A. & Bowen, H.K. (1988). Influence of Various Consolidation Techniques on the Green Microstructure and Sintering Behavior of Alumina Powders, *J. Am. Ceram. Soc.*, Vol. 71, No. 11, (November 1988), pp. (970-977), ISSN 0002-7820.

Sakka, Y. & Hiraga, K. (1999). Preparation Methods and Superplastic Properties of Fine-Grained Zirconia and Alumina Based Ceramics, *Nippon Kagaku Kaishi*, Vol. 8, pp. (497–508), ISSN 0369-4577.

Sigmund, W.M.; Bell, N.S. & Bergström, L. (2000). Novel Powder-Processing Methods for Advanced Ceramics, *J. Am. Ceram. Soc.*, Vol. 83, No. 7, (July 2000), pp. 1557–1574, ISSN 0002-7820.

Suzuki, T.; Sakka, Y.; Nakano, K. & Hiraga, K. (2001). Effect of Ultrasonication on the Microstructure and Tensile Elongation of Zirconia-Dispersed Alumina Ceramics Prepared by Colloidal Processing, *J. Am. Ceram. Soc.*, Vol. 84, No. 9, (September 2001), pp.(2132–2134), ISSN 0002-7820.

Sato, E. & Carry, C. (1995). Effect of Powder Granulometry and Pré-Treatment on Sintering Behavior of Submicron-Grained α-Alumina, *J. Eur. Ceram. Soc.*, Vol. 15, No. 1, pp. (9-16), ISSN 0955-2219.

Searcy, A. W. (1987). Theory for Sintering in Temperature Gradients: Role of Long-Range Mass Transport, *J. Am. Ceram. Soc.*, Vol. 70, No. 3, (March 1987), pp. (C61-C62), ISSN 0002-7820.

Stearns, L. & Harmer, M. P. (1996). Particle-Inhibited Grain Growth in Al_2O_3-SiC: I, Experimental Results, *J. Am. Ceram. Soc.*, Vol. 79, No. 12, (November 1996), pp. (3013-3019), ISSN 0002-7820.

Suryanarayana, C. (1995). Nanocrystalline Materials , *Int. Mat. Reviews*, Vol. 40, No. 2, pp. (41-64), ISSN 0950-6608.

Tartaj, J. & Tartaj, P. (2009). Two-Stage Sintering of Nanosize Pure Zirconia, *J. Am. Ceram. Soc.*, Vol. 92, No. Supplement s1, (January 2009), pp. (S103-S106). ISSN 0002-7820.

Trombini, V.; Pallone, E. M. J. A.; Munir, Z. A. & Tomasi, R. (2007). Spark Plasma Sintering (SPS) de Nanocompósitos de Al_2O_3-ZrO_2, *Cerâmica*, Vol. 53, No. 325 , (Jan-Mar 2007), pp. (62-67), ISSN 0366-6913.

Wang, C. J.; Huang, C. Y. & Wu, Y. C. (2009). Two-step Sintering of Fine Alumina–Zirconia Ceramics, *Ceram. Int.*, Vol. 35, No. 4, (May 2009), pp. (1467-1472), ISSN 0272-8842.

Wang, X. H.; Chen, P. L. & Chen, I. W. (2006a). Two-Step Sintering of Ceramics with Constant Grain-Size, I. Y_2O_3, *J. Am. Ceram. Soc.*, Vol. 89, No 2, (February 2006), pp. (431-437), ISSN 0002-7820.

Wang, X. H.; Deng, X. Y.; Bai, H. I.; Zhou, H.; Qu, W. G.; Li, L.T. & Chen, I.W. (2006b). Two-Step Sintering of Ceramics with Constant Grain-Size, II.BaTiO3 and Ni-Cu-Zn Ferrite, *J. Am. Ceram. Soc.*, Vol. 89, No. 2, (February 2006), pp.(438-443), ISSN 0002-7820.

Weibel, A.; Bouchet, R.; Denoyel, R. & Knauth, P. (2007). Hot Pressing of Nanocrystalline TiO_2 (Anatase) Ceramics with Controlled Microstructure, *J. Eur. Ceram. Soc.*, Vol. 27, No. 7, pp. (2641-2646), ISSN 0955-2219.

Zhou, Y.; Erb, U.; Aust, K. T. & Palumbo, G. (2003). The Effects of Triple Junctions and Grain Boundaries on Hardness and Young Modulus in Nanostructured Ni-P, *Scr. Mater.*, Vol.48, No. 6, (March 2003), pp. (825-830), ISSN 1359-6462.

Zhou, Y.; Hirao, K.; Yamauchi, Y. & Kanzaki, S. (2004). Densification and Grain Growth in Pulse Electric Current Sintering of Alumina, *J. Eur. Ceram. Soc.* Vol. 24, No. 12, pp. (3465-3470), ISSN 0955-2219.

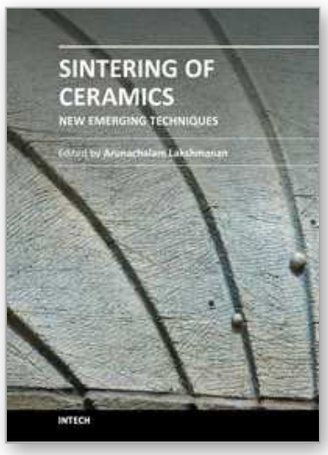

Sintering of Ceramics - New Emerging Techniques
Edited by Dr. Arunachalam Lakshmanan

ISBN 978-953-51-0017-1
Hard cover, 610 pages
Publisher InTech
Published online 02, March, 2012
Published in print edition March, 2012

The chapters covered in this book include emerging new techniques on sintering. Major experts in this field contributed to this book and presented their research. Topics covered in this publication include Spark plasma sintering, Magnetic Pulsed compaction, Low Temperature Co-fired Ceramic technology for the preparation of 3-dimesinal circuits, Microwave sintering of thermistor ceramics, Synthesis of Bio-compatible ceramics, Sintering of Rare Earth Doped Bismuth Titanate Ceramics prepared by Soft Combustion, nanostructured ceramics, alternative solid-state reaction routes yielding densified bulk ceramics and nanopowders, Sintering of intermetallic superconductors such as MgB2, impurity doping in luminescence phosphors synthesized using soft techniques, etc. Other advanced sintering techniques such as radiation thermal sintering for the manufacture of thin film solid oxide fuel cells are also described.

InTech Europe
University Campus STeP Ri
Slavka Krautzeka 83/A
51000 Rijeka, Croatia
Phone: +385 (51) 770 447
Fax: +385 (51) 686 166
www.intechopen.com

InTech China
Unit 405, Office Block, Hotel Equatorial Shanghai
No.65, Yan An Road (West), Shanghai, 200040, China
中国上海市延安西路65号上海国际贵都大饭店办公楼405单元
Phone: +86-21-62489820
Fax: +86-21-62489821

IntechOpen